

A highly conserved basidiomycete peptide synthetase produces a trimeric hydroxamate

siderophore

Eileen Brandenburger,^a Markus Gressler,^{b*} Robin Leonhardt,^{a†} Gerald Lackner,^c Andreas Habel,^d
Christian Hertweck,^d Matthias Brock,^e Dirk Hoffmeister^{a#}

Department of Pharmaceutical Microbiology at the Hans Knöll Institute, Friedrich Schiller
University, Jena, Germany^a;

Department Microbial Biochemistry and Physiology, Leibniz Institute for Natural Product
Research and Infection Biology - Hans Knöll Institute, Jena, Germany^b;

Junior Group Synthetic Microbiology, Friedrich Schiller University, Jena, Germany^c;

Department Biomolecular Chemistry, Leibniz Institute for Natural Product Research and
Infection Biology - Hans Knöll Institute, Jena, Germany^d;

School of Life Sciences, University of Nottingham, United Kingdom^e

Present addresses:

*Markus Gressler, Department of Parasitology and Mycology at the Pasteur Institute, Paris,
France, [†]Robin Leonhardt, Roche Diagnostics, Penzberg, Germany

#Address correspondence to Dirk Hoffmeister, dirk.hoffmeister@leibniz-hki.de.

Running title: Basidiomycete siderophore synthetase

22 **Abstract**

23 The model white-rot basidiomycete *Ceriporiopsis (Gelatoporia) subvermispora* B encodes
24 putative natural product biosynthesis genes. Among them is the gene for the seven-domain
25 nonribosomal peptide synthetase CsNPS2. It is a member of the as-yet uncharacterized fungal
26 type VI siderophore synthetase family which is highly conserved and widely distributed among
27 the basidiomycetes. These enzymes include only one adenylation (A) domain, i.e., one
28 complete peptide synthetase module and two thiolation/condensation (T-C) di-domain partial
29 modules which, together, constitute an AT₁C₁T₂C₂T₃C₃ domain setup. The full-length CsNPS2
30 enzyme (274.5 kDa) was heterologously produced as polyhistidine fusion in *Aspergillus niger* as
31 soluble and active protein. *N*⁵-acetyl-*N*⁵-hydroxy-L-ornithine (L-AHO) and *N*⁵-*cis*-
32 anhydromevalonyl-*N*⁵-hydroxy-L-ornithine (L-AMHO) were accepted as substrates, as assessed
33 *in vitro* using the substrate-dependent [³²P]ATP-pyrophosphate radioisotope exchange assay.
34 Full-length *holo*-CsNPS2 catalyzed amide bond formation between three L-AHO molecules to
35 release the linear L-AHO trimer, called basidioferrin, as product *in vitro*, which was verified by
36 LC-HRESIMS. Phylogenetic analyses suggest that type VI family siderophore synthetases are
37 widespread in mushrooms and have evolved in a common ancestor of basidiomycetes.

38

39

40 **Importance:** The basidiomycete nonribosomal peptide synthetase CsNPS2 represents a
41 member of a widely distributed but previously uninvestigated class (type VI) of fungal
42 siderophore synthetases. Genes orthologous to *CsNPS2* are highly conserved across various

43 phylogenetic clades of the basidiomycetes. Hence, our work serves as a broadly applicable
44 model for siderophore biosynthesis and iron metabolism in higher fungi. Also, our results on
45 the amino acid substrate preference of CsNPS2 supports further understanding of the substrate
46 selectivity of fungal adenylation domains. Methodologically, this report highlights the
47 *Aspergillus niger*/SM-Xpress-based system as suitable platform to heterologously express
48 multimodular basidiomycete biosynthesis enzymes in the > 250 kDa range in soluble and active
49 form.

50

51

52 Introduction

53 The transition element iron plays an essential role for numerous fundamental physiological
54 processes, among them electron transport, e.g., during oxidative phosphorylation and nucleic
55 acid biosynthesis [1,2]. The solubility product for $\text{Fe}(\text{OH})_3$ is 10^{-39} M [2]. To compensate for this
56 very low bioavailability, fungi primarily use high-affinity ferric iron-specific chelating natural
57 products, referred to as siderophores, to acquire iron extracellularly from their environment
58 and for intracellular iron storage and sequestration [1,3]. A second, less efficient acquisition
59 strategy includes enzymatic reductive iron uptake [4]. Structurally, most fungal siderophores
60 belong to the hydroxamate family of compounds (Fig. 1). They share N^5 -acyl- N^5 -hydroxy-L-
61 ornithine as building blocks and chelate ferric iron through octahedral co-ordination to the
62 oxygen atoms of the hydroxy and the acyl groups bound to these modified L-ornithine residues.
63 Siderophores can structurally be further divided into i) the trimeric fusarinines, represented,

64 e.g., by triacetylfusarinine C (TAFC), a secreted siderophore of *Aspergillus fumigatus* [5]), ii) the
65 coprogens [6, 7], iii), the ferrichromes, which include three N^5 -acylated N^5 -hydroxy-L-ornithine
66 units in their usually hexameric structure, represented, e.g., by ferricrocin as intracellular
67 storage siderophore of *Aspergilli* [5,8], and iv) rhodotorulic acid which is a dihydroxamate
68 diketopiperazine [9,10].

69 Fungal siderophore biosynthesis has been studied extensively for *Aspergillus*, *Fusarium*,
70 *Cochliobolus*, and other ascomycete genera [11-14]. The key enzymatic activity to assemble the
71 backbone structure is provided by nonribosomal peptide synthetases (NRPSs). These are
72 exceptionally large modular multi-domain enzymes which catalyze amide bond formation
73 between proteinogenic or non-proteinogenic α -amino acids, or α -keto acids, that are covalently
74 tethered to the enzyme via thioester bonds [15]. Depending on the domain architecture,
75 siderophore-producing NRPSs are grouped into categories type I-VI [3]. Despite different
76 products, all of them share a characteristic terminal thiolation (T)-/condensation (C) didomain
77 duplication or, in most cases, triplication. Discrete enzymes catalyze the reaction to provide
78 siderophore synthetases with monomeric substrates. These steps include monooxygenase-
79 mediated hydroxylation and acylation of the nitrogen atom N^5 of L-ornithine by an
80 acyltransferase.

81 The impressive body of literature on ascomycete siderophores is starkly contrasted by the
82 paucity of data on their basidiomycete congeners, whose genetic or enzymatic requisites for
83 siderophore production are largely unknown. Merely two reports exist that pertain to
84 ferrichrome and ferrichrome A biosynthesis in *Ustilago maydis* [16,17], alongside a report on

85 the identification of ferrichrome A biosynthesis genes in the Jack O'Lantern mushroom
86 *Omphalotus olearius* [18]. A trimeric siderophore, basidiochrome, has been isolated from
87 *Ceratobasidium* and *Rhizoctonia* species [19].

88 Genomic sequencing of basidiomycetes of various phylogenetic clades [20-23] identified
89 strongly conserved genes for a putative seven-domain type VI siderophore synthetase
90 (AT₁C₁T₂C₂T₃C₃, Fig. 2) in numerous species. Dissimilar to other fungal siderophore synthetases,
91 type VI enzymes feature only one adenylation (A) domain, plus the prototypical TC domain
92 triple. Following the biosynthetic logic of NRPSs, this domain configuration should result in a
93 homotrimeric enzymatic product, making this most conserved basidiomycete NRPS
94 incompatible with the biosynthesis of the heterohexameric ferrichromes but potentially
95 consistent with a basidiochrome-like trimer.

96 The siderophore synthetase of the model white-rot basidiomycete *Ceriporiopsis subvermispora*,
97 CsNPS2, is a representative of numerous type VI basidiomycete NRPSs. We here describe its
98 functional *in vitro* characterization, along with the chemical identification of its product.

99

100 RESULTS

101 **Phylogeny of basidiomycete type VI siderophore synthetases.** Numerous basidiomycetes of
102 distinct phylogenetic clades encode strongly conserved genes for putative seven-domain
103 nonribosomal peptide synthetases, making these enzymes one of the most common (if not the
104 most common) basidiomycete NRPS. Although their function has remained unknown, their
105 domain setup points to type VI siderophore synthetases [3]. This study aims at functional

106 characterization of this group of fungal NRPSs. Among countless others, this particular putative
107 NRPS gene (*CsNPS2*) is found in the white-rot model species *Ceriporiopsis subvermispora*,
108 whose genomic sequence has been published [24] and which was chosen as a representative
109 model.

110 A sequence alignment was produced using the MUSCLE algorithm [25]. The first set included A
111 domains which adenylate L-ornithine derivatives and which were taken from characterized
112 asco- and basidiomycete ferrichrome synthetases. The second set represented A domains of
113 *CsNPS2*-like enzymes with A-T-C-T-C-T-C domain set-up. The phylogenetic clustering analysis
114 (Fig. 3) supported the assumption that all *CsNPS2*-like A domains would group together, and
115 represented a monophyletic sub-branch of the tree. This phylogeny extends previous results in
116 which a *CsNPS2*-like protein (EAU88504.2 of *Coprinopsis cinerea*) was categorized as
117 representative of type VI of siderophore synthetases [3]. Type VI family enzymes are exclusively
118 found encoded in basidiomycete genomes and have most likely evolved in an ancient
119 basidiomycete. Notably, all *N*⁵-acyl-*N*⁵-hydroxy-L-ornithine-activating A domains cluster
120 together. Still, they are only remotely related to the ferrichrome A synthetase of the
121 basidiomycete *Omphalotus olearius* [18].

122

123 **Identification of siderophore biosynthesis genes.** The *C. subvermispora* genome harbored two
124 adjacent genes (Fig. 2), encoding a putative monooxygenase (SMO1, 541 aa, calculated mass
125 59.6 kDa, JGI protein ID 113443) and NRPS (*CsNPS2*, 2464 aa, 270.8 kDa, JGI protein ID 153005).
126 These enzymes may be involved in siderophore biosynthesis in *C. subvermispora*. We further

127 identified a gene that encodes a putative siderophore transporter of the major facilitator
128 superfamily (MFS1, protein ID 163556). However, *MFS1* is not clustered with *CsNPS2*. The
129 deduced MFS1 protein (600 aa, 64.4 kDa) shares 36.5 %, 30 %, and 36 % identical amino acids
130 with the characterized transporters MirA, MirB, and MirC of *A. nidulans* [7, 26]. The *CsNPS2*
131 gene is interrupted by 14, *SMO1* by five, and the *MFS* gene by 12 introns. A comparably
132 clustered arrangement of genes for a monooxygenase and an NRPS is found with various fungi,
133 e.g., for ferrichrome A biosynthesis in the basidiomycete *Omphalotus olearius* [18], whereas the
134 transporter genes do usually not cluster with the siderophore synthetase gene. Automatic
135 annotation identified *SMO1* as putative L-ornithine *N*⁵-monooxygenase that contains a
136 Rossmann-fold for NADPH+H⁺ binding. *SMO1* is similar (49% identical aa) to *Aspergillus*
137 *fumigatus* SidA, which catalyzes the first step of the ferricrocin/fusarinine C biosynthesis [27].
138 *CsNPS2* resembles a trimodular siderophore synthetase that includes an adenylation domain
139 and a triplicated thiolation-condensation di-domain (Fig. 2). Such triplications are also found
140 with *Aspergillus fumigatus* SidC and numerous other siderophore synthetases [3,28]. However,
141 *CsNPS2* and *CsNPS2*-like enzymes of other basidiomycetes (Table 1) are dissimilar from SidC in
142 that only one A domain is present.

143

144 **Iron-dependent expression of natural product biosynthesis genes.** The expression of
145 siderophore biosynthesis genes is upregulated in response to iron limitation [4], e.g., shown for
146 *sidC* and *sidA* of *A. fumigatus* [29]. Therefore, our hypothesis that *CsNPS2* and *SMO1* serve
147 siderophore biosynthesis in *C. subvermispota*, was initially tested by a semi-quantitative

148 reverse-transcription PCR. We used cDNA obtained from cultures grown under high iron
149 conditions (that is, 10 μM FeCl_2) or iron-depleted conditions, i.e., without iron, but with 200 μM
150 of the ferrous iron chelator bathophenanthrolinedisulfonic acid (BPS) (Fig. S1). The
151 constitutively expressed glyceraldehyde-3-phosphate dehydrogenase gene (*GDH*) served as
152 reference. The transcripts of *CsNPS2*, *SMO1*, and *MFS1* were more pronounced in cultures
153 grown under iron-deplete conditions. This finding is consistent with the hypothesis that
154 *CsNPS2*, *SMO1*, and *MFS1* may produce and transport siderophores. Further evidence for
155 siderophore secretion by *C. subvermispota* derived from the CAS-based siderophore detection
156 assay. When the fungus was grown in the modified CAS assay using split plates (half CAS agar,
157 half MEP, Fig. S2), a pale yellow area on the CAS side of the contact zone between the two
158 media indicated siderophore secretion by *C. subvermispota* under iron deplete conditions.

159

160 ***In silico* analysis of CsNPS2 substrate specificity.** To characterize the substrate specificity of
161 *CsNPS2 in vitro*, we determined its nonribosomal code. It comprises ten mostly non-adjacent
162 amino acids in adenylation domains that line the substrate-binding pocket and, thus, impact
163 substrate preference. We identified the aa motif D-V-A-G-A-G-F-I-G-K in *CsNPS2*, which is also
164 present in *CsNPS2*-like enzymes of other basidiomycetes in identical or near-identical form
165 (Table 1). With an aspartic acid residue on the first position (D235, numbering according to the
166 bacterial reference enzyme PheA [30]), this code indicates that an α -amino acid is the preferred
167 *CsNPS2* substrate. Crystallography proved this aspartic acid residue as critical to stabilize the α -
168 amino group of the substrate [31]. Further, the *CsNPS2* code resembles to some degree that for

169 L-AHO-activating domains. For instance, the code D-V-L-D-I-G-F-I-G-K was found in the *N*⁵-
170 acetyl-*N*⁵-hydroxy-L-ornithine-activating A domain of the ferrichrome synthetase Sib1 of
171 *Schizosaccharomyces pombe* [28]. Notably, based on the crystal structure of the *Neotyphodium*
172 *lolii* epichloënin synthetase SidN (pdb: 3ITE), an extended specificity code for L-AHO activating
173 domains was proposed [32]. However, the relevance for substrate prediction by basidiomycete
174 A domains remains still elusive.

175

176 ***In vitro* analysis of CsNPS2 substrate specificity.** Next, we determined the substrate specificity
177 of the CsNPS2 A domain *in vitro*. A total of 24 amino acid substrates were tested, including
178 *N*⁵-hydroxy-L-ornithine, L-AHO, and L-AMHO. Heterologous production of the full-length and *N*-
179 terminally hexahistidine-tagged 274.5 kDa CsNPS2 protein was accomplished in *Aspergillus*
180 *niger* tEB09. Protein purification was performed by metal affinity chromatography and verified
181 by SDS-polyacrylamide gel electrophoresis (Fig. S3). Pure CsNPS2 was assayed by substrate-
182 dependent ATP-[³²P]-pyrophosphate radiolabel exchange. High turnover was detected for
183 monomeric siderophore building blocks L-AHO (919,700 cpm, Fig. 4) and L-AMHO (879,800
184 cpm). Contrastingly, poor activity was observed for L-ornithine and L-alanine (3,640 and 4,050
185 cpm, respectively), i.e., values which are as low as the negative control with water as substrate
186 (1,930 cpm).

187

188 **Natural product analysis of *C. subvermispora* cultures.** CsNPS2 includes only a single A domain.
189 Following the biosynthetic logic of NRPSs, only one monomeric substrate species would thus be

190 loaded onto the T domains through repetitive A-domain activity, followed by amide bond
191 formation between monomers. Consequently, this domain set-up makes a function as
192 synthetase for ferrichrome, ferricrocin, or ferrirhodin unlikely, but points to a homotrimeric
193 compound, such as des(diserylglycl)ferrirhodin [33] or fusarinine B [34] (Fig. 1). Mycelial
194 extracts and the culture broth of *C. subvermispora*, grown under iron-limiting conditions, were
195 chromatographically analyzed. Considering the A domain's specificity for L-AHO and L-AMHO
196 and given that the relevant sequence portion (²¹³⁶LHHFQYDAWS²¹⁴⁵) of the terminal C domain
197 of CsNPS2 does not feature the signature motif typical for fungal C domain-like cyclization
198 domains [35], a linear CsNPS2 trimeric product was anticipated. While the CAS agar diffusion
199 assay indicated iron-chelating properties of XAD-16 extracts, the expected masses of L-AHO and
200 L-AMHO trimers (linear or cyclic) were not detected. We therefore conclude that a linear
201 homotrimer from either of these starter units does not represent the ultimate pathway product
202 in *C. subvermispora*. Likely, it undergoes further post-NRPS modification, e.g., glycosylation, as
203 shown for *Metarhizium robertsii* metachelins [36] or bacterial enterobactins [37], or acetylation
204 or hydroxylation which are found, e.g., with *Aspergillus fumigatus* ferricrocins [38].

205

206 **CsNPS2 product formation *in vitro*.** Given the difficult siderophore identification *in vivo*, we
207 followed an *in vitro* approach and performed product formation assays for the definitive
208 functional characterization of CsNPS2. For most basidiomycetes, including *C. subvermispora*
209 transformation and genetic manipulation is not established and reverse genetics is not an
210 option. For *in vitro* assays, we used either 1 mM L-AHO or L-AMHO as amino acid substrate. The

211 reactions proceeded for 24 h and were again analyzed by the CAS agar diffusion assay. Only the
212 reaction with the substrate L-AHO resulted in a color change in the CAS agar from blue to yellow
213 which indicated the formation of a Fe(III)-chelating product (Fig. S2). When L-AMHO was
214 offered as substrate or when ATP was omitted (negative control), the CAS assays did not
215 indicate iron chelation. Further analysis by HPLC and high-resolution mass spectrometry
216 detected a signal at $t_R = 8.3$ min, which was not present in the negative control (Fig. 5). High
217 resolution mass spectrometry revealed a compound with m/z 535.2719 $[M+H]^+$, which is
218 consistent with the iron-void linear trimer of L-AHO, now referred to as basidioferrin
219 ($C_{21}H_{38}N_6O_{10}$; calculated m/z 535.2722 $[M+H]^+$), and a compound with m/z 588.1840 which is
220 consistent with the $^{56}Fe^{3+}$ complex ($C_{21}H_{35}N_6O_{10}Fe$, calculated m/z 588.1839 $[M+H]^+$). In the
221 assay with L-AMHO as substrate, product formation was not detected. The *in vitro* results
222 confirmed the above predictions made *in silico* and confirm the view that CsNPS2 acts as
223 siderophore synthetase.

224

225 DISCUSSION

226 The enzymatic and genetic basis of basidiomycete siderophore biosynthesis is still
227 underexplored, compared to ascomycetes. Besides the above-mentioned results on *Ustilago*
228 and *Omphalotus ferrichromes*, trimeric N^5 -(3-methyl-*cis*-glutaconyl)- N^5 -hydroxy-L-ornithine,
229 referred to as basidiochrome, was reported from *Ceratobasidium* and *Rhizoctonia* species [19].
230 For the ectomycorrhiza fungus *Suillus granulatus*, production and secretion of fusarinines B and
231 C (=linear and cyclic fusigen, respectively), ferrichrome, coprogen, and TAFC have been

232 reported. Similarly, the closely related mushroom *Suillus luteus* was found to release fusarinine
233 B and fusarinine C (=fusigen), ferricrocin, and coprogen [39] (Fig. 1). However, these findings
234 are inconsistent with genomic data as neither species encodes a ferrichrome synthetase, a
235 SidC-like enzyme that would provide the catalytic capacity to synthesize TAFC, or an enzyme
236 that is consistent with coprogen biosynthesis. However, the above *Suillus* species encode a
237 CsNPS2-type siderophore synthetase. Whereas both L-AHO and L-AMHO are adenylated by the
238 CsNPS2 A domain, our results demonstrate that only the former is trimerized. Assuming equal A
239 domain preferences in the *Suillus* synthetases, but L-AMHO as the sole building block that
240 undergoes trimerization, our biochemical data could be well reconciled with the previously
241 observed fusarinine B production. Its biosynthesis also appears plausible, as a linear trimeric N^5 -
242 acylated N^5 -hydroxy-L-ornithine with chelating properties represents the immediate product of
243 the respective enzyme.

244 CsNPS2 comprises only one single A domain, which is consistent with the enzyme's
245 homotrimeric product, yet implies repeated A domain activity to load all T domains with
246 monomeric L-AHO. The phenomenon of iterative loading is, however, reminiscent of other
247 siderophore synthetases, e.g., in *Schizosaccharomyces pombe* [28] or during yersiniabactin
248 biosynthesis [40]. Our work on CsNPS2 was focused on the biochemical characterization of a
249 type VI siderophore synthetase, i.e., a previously uninvestigated class of basidiomycete
250 enzymes. The finding that its A domain accepts both L-AHO and L-AMHO as monomers, but
251 oligomerizes only the former, is remarkable and contrasts the situation of siderophore
252 biosynthesis in the ascomycete *Aspergillus fumigatus*, which has been profoundly investigated

253 for its iron metabolism. This fungus has two siderophore synthetases, i.e., SidD for TAFC
254 production and SidC to synthesize ferricrocin, respectively [5]. While the former synthetase is
255 strictly specific for L-AMHO, the latter accepts L-AHO as chelating building block. Another
256 interesting observation on *C. subvermispora* CsNPS2 is that the gene is not only transcribed
257 under iron depletion, but also, though at lower levels, in the presence of iron. Taking into
258 account that no other obvious gene coding for siderophores had been detected in the *C.*
259 *subvermispora* genome, this may point to a second function as intracellular storage
260 siderophore, besides extracellular iron acquisition. This would be dissimilar to *A. fumigatus*,
261 which uses separate molecules, ferricrocin *versus* TAFC and fusarinine C, to fulfill these
262 functions [5].

263

264 In conclusion, numerous basidiomycete genomes of various phylogenetic clades and lifestyles
265 code for seven-domain type VI siderophore synthetases. Hence, our work on CsNPS2 has pilot
266 character and helps investigate and understand iron metabolism in basidiomycetes more
267 thoroughly and comprehensively.

268

269 MATERIALS AND METHODS

270 **General.** Standard molecular biology procedures were performed as described [41]. Isolation of
271 plasmid DNA from *Escherichia coli*, restriction and ligation followed the instructions of the
272 manufacturers of kits and enzymes (NEB, Promega, Fermentas, Thermo Fisher Scientific, and
273 Zymo Research). Chemicals and media components were purchased from Becton-Dickinson,

274 Fisher, Fluka, Novagen, Roth, Sigma-Aldrich, and Takara. The sodium salt of [³²P]pyrophosphate
275 was from PerkinElmer.

276

277 **Microorganisms and cultivation.** Routine cloning was done in *E. coli* XL1 blue. *E. coli* BL21(DE3)
278 and SoluBL were used for heterologous protein production. *E. coli* was cultured in LB- or
279 overnight express instant TB medium, amended with kanamycin (50 µg/ml) or carbenicillin (50
280 µg/ml) for selection. *Ceriporiopsis subvermispota* [24] was grown at room temperature on malt
281 extract peptone (MEP) agar (per liter: 30 g malt extract, 3 g soy peptone, 18 g agar, pH 5.6).
282 Seed cultures were grown in liquid MEP medium, for main cultures, low iron medium (LIM) [19]
283 was used. To induce siderophore biosynthesis, 200 µM bathophenanthroline disulfonic acid
284 (BPS) disodium salt was added. *Aspergillus niger* P2 [42] and its derivative tEB09 (*PamyB:terR*;
285 *PterA:NPS2*, this study) were grown on *Aspergillus* minimal medium (AMM + 100 mM D-glucose
286 and 70 mM NaNO₃) [43] containing 2 % agar, or as liquid seed culture with 100 mM D-glucose,
287 at 30 °C. Pyrithiamine hydrobromide (0.1 µg/ml) and phleomycin (80 µg/ml) were added, if
288 appropriate.

289

290 **cDNAs synthesis and plasmid construction.** RNA isolation was carried out with the SV Total
291 RNA Isolation kit (Promega). Reverse transcription PCR in a total volume of 20 µl (60 min; 42 °C)
292 was used to produce cDNA. To amplify a partial gene encoding the A₁-T₁-didomain of
293 *C. subvermispota* *CsNPS2* (putative siderophore synthetase gene), the first-strand synthesis
294 reaction was primed with oligonucleotide NPS2-1 (1 µM, Table 2), 2.5 mM MgCl₂, 0.5 mM each

295 dNTP, 1 μ g total RNA, and ImProm-II reverse transcriptase (Promega). Subsequently, 1 μ l of the
296 first strand reaction was used as template in a standard PCR. The reaction included 0.2 mM
297 each dNTP, 0.5 μ M (each) oligonucleotides NPS2fw and NPS2rev (Table 2), and 2 units *Pfu* DNA-
298 polymerase (Promega), in the buffer provided with the enzyme, in a total volume of 50 μ l.
299 Thermocycling parameters were: initial denaturation, 30 s, 94 $^{\circ}$ C; amplification, 35 cycles (94 $^{\circ}$ C
300 for 30 s, 58 $^{\circ}$ C for 30 s, 72 $^{\circ}$ C for 6 min 30 s); terminal hold, 5 min at 72 $^{\circ}$ C. The purified PCR
301 product was restricted with *Bam*HI and *Eco*RI, whose recognition sites were introduced by the
302 above primers, and ligated to the vector pBSK, restricted equally, to create plasmid pRL1 (see
303 Fig. S4 for plasmid construction). The insert was then ligated into vector pRSETb, using the
304 same restriction sites, to create expression plasmid pRL3. The *CsNPS2* full-length gene was
305 reconstituted by amplifying the portion between its naturally occurring *Sac*II site and the stop
306 codon with primers oRL1 and oRL2 (Table 2, PCR parameters as mentioned before), restriction
307 of the amplicon by *Sac*II and *Mfe*I, and ligation into pRL3, restricted by *Sac*II and *Eco*RI, to yield
308 plasmid pRL5.

309 The full-length *CsNPS2* reading frame was then ligated to the SM-Xpress vector [42] by *in vitro*
310 recombination, using the InFusion HD Cloning Kit (Clontech), to create plasmid pEB16. To this
311 end, the gene was amplified by PCR (total volume 10 μ l), using 20 ng pRL5 as template, 0.2 mM
312 each dNTP, 1 μ M each oligonucleotide (oEB28/oEB30, Table 2), and 1 unit Phusion DNA
313 polymerase, in the GC-buffer provided with the enzyme. Thermal speedcycling parameters
314 were: initial denaturation at 98 $^{\circ}$ C for 30 s; amplification with 33 cycles (98 $^{\circ}$ C for 7 s, 61 $^{\circ}$ C for 7
315 s, 72 $^{\circ}$ C for 125 s); terminal hold, 5 min at 72 $^{\circ}$ C.

316

317 **Semi-quantitative PCR.** Total RNA was isolated from *C. subvermispora* mycelia cultivated under
318 high iron (10 μ M FeSO₄) and iron-deplete conditions (no iron, with 200 μ M BPS). cDNA
319 synthesis was performed with 500 ng template RNA per reaction. Semi-quantitative PCR was
320 carried out with primer pairs (0.5 μ M each) oRL3/oRL4 (for *CsNPS2*, the putative siderophore
321 synthetase, KY287598), oEB48/oEB49 (*MFS1*, putative siderophore transporter gene,
322 EMD31052.1), oEB54/oEB55 (*SMO1*, putative monooxygenase gene, EMD38274.1) and
323 oEB46/oEB47, (*GDH1*, glyceraldehyde-3-phosphate dehydrogenase gene, EMD35149.1), in
324 which the latter served as reference standard. Oligonucleotide sequences are shown in Table 2.
325 Thermal cycling parameters were: 30 s at 98 °C; 27 cycles of 98 °C for 10 s, 54 °C for 15 s and
326 72 °C for 105 s, followed by a terminal hold for 5 min at 72 °C. The PCR products were
327 separated by agarose gel electrophoresis.

328

329 ***Aspergillus niger* transformation and heterologous gene expression.** *A. niger* P2 (=FGSC
330 A1144_ *PamyB:terR*) [42] was transformed with plasmid pEB16. Conidia (1×10^7 in 50 ml AMM)
331 were inoculated and incubated on an orbital shaker at 120 rpm and 30 °C overnight. Mycelium
332 was harvested and washed with 100 ml YAT buffer (0.6 M KCl, 50 mM maleic acid, pH 5.5). For
333 protoplast formation, mycelium was incubated with 100 mg Yatalase and 100 mg lysing enzyme
334 in 20 ml YAT buffer for approximately 2 h (30 °C, 70 rpm). Protoplasts were filtered and washed
335 three times with wash solution (0.6 M KCl, 0.1 M Tris-HCl, pH 7.0). Protoplasts were then
336 resuspended in solution A (0.6 M KCl, 50 mM CaCl₂, 10 mM Tris-HCl, pH 7.5) to give a final

337 concentration of 5×10^7 to 2×10^8 protoplasts/ml. To 100 μ l protoplast suspension, 1-20 μ g
338 plasmid DNA was added, followed by incubation on ice for 5 min. After addition of 25 μ l PEG
339 solution (25 % (w/v) PEG 8000, 50 mM CaCl_2 , 10 mM Tris-HCl, pH 7.5) the mixture was kept on
340 ice for further 20 min. Then, another 500 μ l of PEG solution was added. After incubation on ice
341 for further 5 min, 1 ml solution A was added. 400 μ l of the transformation reaction was mixed
342 with 12 ml top agar (AMM, 50 mM D-glucose, 1.2 M sorbitol, 80 μ g/ml phleomycin, 2 % agar,
343 pH 6.5) and poured onto agar plates of the same composition. Plates were cultured at 30 °C for
344 3-5 days. Conidia from colonies were transferred four times to fresh plates. A PCR-based pre-
345 screen with primers 2641 and 2644 (Table 2) was used to test for full-length transgene
346 integration. Genomic DNAs of nine pre-selected transformants were subsequently tested for
347 single-integration events of the *CsNPS2* cassette (*PterA:Csnps2:trpC^T*) by Southern blotting,
348 using a 0.9 kb digoxigenin-labeled *CsNPS2*-specific probe (DIG high prime, Roche, Fig. S5). For
349 visualization, blots were treated with CDP-star, according to the manufacturer's instruction
350 (Roche). A transformant (*A. niger* tEB09) with a single integration of the expression construct in
351 the genome was used for further work.

352

353 **Protein purification.** Heterologous production of *Streptomyces verticillus* phosphopantetheinyl
354 transferase Svp in *E. coli* BL21(DE3) was performed as previously described [44]. Cells were
355 harvested by centrifugation (4 °C, 3,200 \times g, 20 min), and the cell paste was resuspended in lysis
356 buffer (50 mM $\text{NaH}_2\text{PO}_4 \times \text{H}_2\text{O}$, 300 mM NaCl, 10 mM imidazole, pH 8.0), followed by sonication
357 to disrupt cells, centrifugation to remove debris, and FPLC-based purification (see below).

358 To produce full-length CsNPS2, conidia of *A. niger* tEB09 (1×10^6 in 50 ml) were used to
359 inoculate AMM+100 mM D-glucose+70 mM NaNO₃, at 30 °C and 200 rpm, for 48 h. The
360 mycelium was harvested, ground under liquid nitrogen and resuspended in buffer (50 mM Tris,
361 150 mM NaCl, pH 8.0). Cell debris was removed by centrifugation (4 °C, 14,000 × g, 20 min).
362 An Äkta Pure FPLC instrument (GE Healthcare) was used for immobilized metal affinity
363 chromatography. The instrument was equipped with a 1 ml His-Trap FF crude column (GE
364 Healthcare). Buffer A (50 mM NaH₂PO₄, 300 mM NaCl, pH 7.5) and buffer B (500 mM imidazole
365 in buffer A) were used as mobile phase. The wash was performed with a step gradient (5-12 %
366 B, equivalent to 25-60 mM imidazole) within 10 min. Elution of the histidine-tagged target
367 proteins (CsNPS2 full-length, Svp) was carried out at 100 % B. Proteins were desalted on a PD-
368 10 column (GE Healthcare) and eluted with buffer (80 mM Tris-HCl, 5 mM MgCl₂, 100 μM EDTA,
369 pH 7.5). Protein purification was verified on polyacrylamide gels, the protein concentration was
370 determined by Bradford's assay [45]. Additional MALDI-TOF/TOF MS analysis confirmed the
371 authenticity of CsNPS2.

372

373 **Siderophore detection assay.** Siderophore activity was detected by the Chrome Azurol S (CAS)
374 agar diffusion method as described [46,47] and used to characterize the *in vitro* product of
375 CsNPS2. A 35 μl sample of the assay was filled into a 5 mm-diameter well. The plate was
376 incubated for 4 h at 37 °C. For analyses of siderophores produced *in vivo*, a split plate [48] was
377 used consisting of one half CAS agar for siderophore detection, and one half MEP agar, on
378 which the fungus was grown.

379

380 **Radiolabel exchange assay.** The substrate preferences of the CsNPS2 A domain was
381 determined by the substrate-dependent ATP-[³²P]pyrophosphate radiolabel exchange assay. All
382 reactions were run in triplicates. The reactions consisted of 80 mM Tris-buffer, 5 mM MgCl₂, 5
383 mM ATP, 1 mM substrate, 100 nM purified enzyme, and 0.1 μM [³²P]pyrophosphate (50
384 Ci/mmol). Substrates were: all proteinogenic L-amino acids, glycine, as well as L-ornithine,
385 N⁵-hydroxy-L-ornithine, N⁵-acetyl-N⁵-hydroxy-L-ornithine (L-AHO), and N⁵-cis-
386 anhydromevalonyl-N⁵-hydroxy-L-ornithine (L-AMHO, fusarinine). First, substrates were added in
387 pools (Table S1). Components of positive pools were assayed individually. Turnover was
388 determined between 5 °C and 40 °C, and between pH 6 and pH 8. For optimum turnover, the
389 assays were kept at pH 7.5 and 28 °C. The reaction volume was 100 μl. After 30 min, the
390 reactions were stopped and further processed as described [48]. Radiolabel exchange was
391 quantified on a PerkinElmer TriCarb 2910TR scintillation counter.

392

393 **Phosphopantetheinylation of CsNPS2.** For CsNPS2-catalyzed product formation *in vitro*, the
394 phosphopantetheinyl transferase Svp [44] was used to convert *apo*-CsNPS2 into its *holo*-form.
395 100 nM purified CsNPS2, 50 nM Svp, 250 μM coenzyme A in reaction buffer (80 mM Tris-HCl,
396 pH 7.5, 5 mM MgCl₂, 100 μM EDTA) in a total volume of 3 ml were incubated for 30 min at 37
397 °C.

398

399 ***In vitro* product formation.** For CsNPS2-catalyzed product formation, 5 mM ATP and
400 1 mM L-AHO, solved in Tris-HCl buffer (pH 7.5, final volume 2 ml) were added. The reaction was
401 carried out at 28 °C for 24 h, and stopped by lyophilization. The product was solved in
402 methanol, filtered, and analyzed by CAS agar diffusion assay, high performance liquid
403 chromatography (HPLC) and mass spectrometry (LC-MS, see below). For negative control, an
404 ATP-void reaction was run in parallel. To detect iron-loaded siderophore by LC-MS, the assay
405 was split, and 1 mM (final) FeCl₃ was added to one part of the assay.

406

407 **Chemical analysis.** HPLC and LC-MS with *in vitro* products were carried out on an Agilent
408 Infinity 1260 liquid chromatograph equipped with a Zorbax Eclipse XDB-C18 column (150 × 4.6
409 mm, 5 µm particle size) and coupled to a 6130 single quad mass detector. Solvent A was 0.1 %
410 (v/v) formic acid in water, solvent B was acetonitrile. Diode array detection was at λ = 210 nm.
411 The gradient was: 10 % to 20 % B within 15 min, increase to 50 % B in 15 min, from 50 % to 60
412 % B in 10 min, and to 100 % B in another 10 min. For *in vivo* analyses, *Ceriporiopsis*
413 *subvermispora* culture supernatants were filtered and supplemented with Amberlite XAD-16
414 adsorber resin (10 % w/v). The beads were then washed with water, and the elution was
415 performed with 100 % MeOH. Subsequently, the solvent and residual water were removed by
416 rotary evaporation under reduced pressure. The dry extract was resuspended in MeOH. The
417 extract (2 ml) was further fractionated by solid phase extraction using Waters SepPak cartridges
418 (20 ml, C18, 5 g). The step gradient was 10 % to 100 % MeOH in 10 % increments. Fractions
419 were analyzed by the CAS diffusion assay, and CAS assay-positive fractions were analyzed by LC-

420 MS. High-resolution mass spectra were acquired on a Thermo Accela liquid chromatograph with
421 a C18 column (Grom-Sil 100 ODS-0 AB, 250 × 4.6 mm, 3 μm), interfaced to an Exactive Orbitrap
422 spectrometer, operated in positive and negative mode and by electrospray ionization. The
423 following gradient was used: initial hold at 5% B for 1 min, followed by a linear gradient to 100%
424 B within 15 min.

425

426 **Bioinformatic analysis.** The alignment and phylogenetic tree were created with MEGA5
427 software [50] using the built-in muscle alignment engine [25] and the neighbor-joining
428 algorithm. PheA from *Brevibacillus brevis* (pdb:1AMU) [30] was defined as an outgroup. The
429 muscle alignment was further used to determine the nonribosomal specificity codes by
430 extracting alignment positions corresponding to specificity-conferring residues of PheA or SidN3
431 [32].

432

433 **Chemical synthesis.** L-AHO was synthesized from *N*²-benzyloxycarbonyl-L-ornithine and
434 deprotected by hydrogenolysis, following a described procedure [51]. L-AMHO was obtained by
435 mild alkaline hydrolysis of fusarinine C. The identity of both compounds was confirmed using
436 high-resolution mass spectrometry, carried out on the Thermo Exactive instrument mentioned
437 above, and by NMR spectroscopy, performed on a Bruker Avance III 500 MHz spectrometer.

438

439 **ACKNOWLEDGMENTS**

440 We gratefully acknowledge Julia Gressler (Friedrich Schiller University Jena), Maria Poetsch, and
441 Andrea Perner (both Leibniz Institute for Natural Product Research and Infection Biology – Hans
442 Knöll Institute, Jena) for excellent technical assistance. Fusarinine C was kindly provided by
443 Professor Hubertus Haas, Ph.D. (Innsbruck Medical University, Innsbruck, Austria). The authors
444 declare that competing interests do not exist.

445

446 FUNDING INFORMATION

447 This work was supported by the Deutsche Forschungsgemeinschaft (DFG grant HO2515/6-1).

448

449 REFERENCES

- 450 1. **Haas H.** 2003. Molecular genetics of fungal siderophore biosynthesis and uptake: the
451 role of siderophores in iron uptake and storage. *Appl Microbiol Biotechnol* **62**:316-330.
- 452 2. **Hider RC, Kong X.** 2010. Chemistry and biology of siderophores. *Nat Prod Rep* 2010
453 27:637-657.
- 454 3. **Bushley KE, Ripoll DR, Turgeon BG.** 2008. Module evolution and substrate specificity of
455 fungal nonribosomal peptide synthetases involved in siderophore biosynthesis. *BMC*
456 *Evol Biol* **8**:328.
- 457 4. **Haas H.** 2012. Iron - A Key Nexus in the Virulence of *Aspergillus fumigatus*. *Front*
458 *Microbiol* **3**:28.

- 459 5. Schrettl M, Bignell E, Kragl C, Sabiha Y, Loss O, Eisendle M, Wallner A, Arst HN, Jr.,
460 Haynes K, Haas H. 2007. Distinct roles for intra- and extracellular siderophores during
461 *Aspergillus fumigatus* infection. PLoS Pathog **3**:1195-1207.
- 462 6. Winkelmann G, Barnekow A, Ilgner D, Zähler H. 1973. Metabolic products of
463 microorganisms. 120. Uptake of iron by *Neurospora crassa*. Arch Mikrobiol **92**:285-300.
- 464 7. Gressler M, Meyer F, Heine D, Hortschansky P, Hertweck C, Brock M. 2015. Phytotoxin
465 production in *Aspergillus terreus* is regulated by independent environmental signals.
466 eLife **4**: doi: 10.7554/eLife.07861.
- 467 8. Eisendle M, Oberegger H, Zadra I, Haas H. 2003. The siderophore system is essential for
468 viability of *Aspergillus nidulans*: functional analysis of two genes encoding L-ornithine
469 *N*⁵-monooxygenase (*sidA*) and a non-ribosomal peptide synthetase (*sidC*). Mol Microbiol
470 **49**:359-375.
- 471 9. Atkin CL, Neilands JB. 1968. Rhodotorulic acid, a diketopiperazine dihydroxamic acid
472 with growth-factor activity. I. Isolation and characterization. Biochemistry **7**:3734-3739.
- 473 10. Anke T, Diekmann H. 1972. Biosynthesis of sideramines in fungi. Rhodotorulic acid
474 synthetase from extracts of *Rhodotorula glutinis*. FEBS Lett **27**:259-262.
- 475 11. Haas H, Eisendle M, Turgeon BG. 2008. Siderophores in fungal physiology and virulence.
476 Annu Rev Phytopathol **46**:149-187.
- 477 12. Haas H. 2014. Fungal siderophore metabolism with a focus on *Aspergillus fumigatus*.
478 Nat Prod Rep **31**:1266-1276.

- 479 13. **Munawar A, Marshall JW, Cox RJ, Bailey AM, Lazarus CM.** 2013. Isolation and
480 characterisation of a ferrirhodin synthetase gene from the sugarcane pathogen
481 *Fusarium sacchari*. ChemBioChem **14**:388-394.
- 482 14. **Turgeon BG, Oide S, Bushley K.** 2008. Creating and screening *Cochliobolus*
483 *heterostrophus* non-ribosomal peptide synthetase mutants. Mycol Res **112**:200-206.
- 484 15. **Finking R, Marahiel MA.** 2004. Biosynthesis of nonribosomal peptides. Annu Rev
485 Microbiol **58**:453-488.
- 486 16. **Yuan WM, Gentil GD, Budde AD, Leong SA.** 2001. Characterization of the *Ustilago*
487 *maydis* *sid2* gene, encoding a multidomain peptide synthetase in the ferrichrome
488 biosynthetic gene cluster. J Bacteriol **183**:4040-4051.
- 489 17. **Winterberg B, Uhlmann S, Linne U, Lessing F, Marahiel MA, Eichhorn H, Kahmann R,**
490 **Schirawski J.** 2010. Elucidation of the complete ferrichrome A biosynthetic pathway in
491 *Ustilago maydis*. Mol Microbiol **75**:1260-1271.
- 492 18. **Welzel K, Eisfeld K, Antelo L, Anke T, Anke H.** 2005. Characterization of the ferrichrome
493 A biosynthetic gene cluster in the homobasidiomycete *Omphalotus olearius*. FEMS
494 Microbiol Lett **249**:157-163.
- 495 19. **Haselwandter K, Passler V, Reiter S, Schmid DG, Nicholson G, Hentschel P, Albert K,**
496 **Winkelmann G.** 2006. Basidiochrome - a novel siderophore of the Orchidaceous
497 Mycorrhizal Fungi *Ceratobasidium* and *Rhizoctonia* spp. Biometals **19**:335-343.
- 498

- 499 20. Floudas D, Binder M, Riley R, Barry K, Blanchette RA, Henrissat B, Martinez AT, Otilar
500 R, Spatafora JW, Yadav JS, Aerts A, Benoit I, Boyd A, Carlson A, Copeland A, Coutinho
501 PM, de Vries RP, Ferreira P, Findley K, Foster B, Gaskell J, Glotzer D, Gorecki P,
502 Heitman J, Hesse C, Hori C, Igarashi K, Jurgens JA, Kallen N, Kersten P, Kohler A, Kues
503 U, Kumar TK, Kuo A, LaButti K, Larrondo LF, Lindquist E, Ling A, Lombard V, Lucas S,
504 Lundell T, Martin R, McLaughlin DJ, Morgenstern I, Morin E, Murat C, Nagy LG, Nolan
505 M, Ohm RA, Patyshakuliyeva A, Rokas A, Ruiz-Dueñas FJ, Sabat G, Salamov A,
506 Samejima M, Schmutz J, Slot JC, St John F, Stenlid J, Sun H, Sun S, Syed K, Tsang A,
507 Wiebenga A, Young D, Pisabarro A, Eastwood DC, Martin F, Cullen D, Grigoriev IV,
508 Hibbett DS. 2012. The Paleozoic origin of enzymatic lignin decomposition reconstructed
509 from 31 fungal genomes. *Science* **336**:1715-1719.
- 510 21. Eastwood DC, Floudas D, Binder M, Majcherczyk A, Schneider P, Aerts A, Asiegbu FO,
511 Baker SE, Barry K, Bendiksby M, Blumentritt M, Coutinho PM, Cullen D, de Vries RP,
512 Gathman A, Goodell B, Henrissat B, Ihrmark K, Kauserud H, Kohler A, LaButti K,
513 Lapidus A, Lavin JL, Lee YH, Lindquist E, Lilly W, Lucas S, Morin E, Murat C, Oguiza JA,
514 Park J, Pisabarro AG, Riley R, Rosling A, Salamov A, Schmidt O, Schmutz J, Skrede I,
515 Stenlid J, Wiebenga A, Xie X, Kües U, Hibbett DS, Hoffmeister D, Högberg N, Martin F,
516 Grigoriev IV, Watkinson SC. 2011. The plant cell wall-decomposing machinery underlies
517 the functional diversity of forest fungi. *Science* **333**:762-765.
- 518 22. Stajich JE, Wilke SK, Ahrén D, Au CH, Birren BW, Borodovsky M, Burns C, Canbäck B,
519 Casselton LA, Cheng CK, Deng J, Dietrich FS, Fargo DC, Farman ML, Gathman AC,

- 520 Goldberg J, Guigó R, Hoegger PJ, Hooker JB, Huggins A, James TY, Kamada T, Kilaru S,
521 Kodira C, Kües U, Kupfer D, Kwan HS, Lomsadze A, Li W, Lilly WW, Ma LJ, Mackey AJ,
522 Manning G, Martin F, Muraguchi H, Natvig DO, Palmerini H, Ramesh MA, Rehmeier CJ,
523 Roe BA, Shenoy N, Stanke M, Ter-Hovhannisyan V, Tunlid A, Velagapudi R, Vision TJ,
524 Zeng Q, Zolan ME, Pukkila PJ. 2010. Insights into evolution of multicellular fungi from
525 the assembled chromosomes of the mushroom *Coprinopsis cinerea* (*Coprinus cinereus*).
526 Proc Natl Acad Sci USA **107**: 11889-11894.
- 527 23. Shah F, Nicolás C, Bentzer J, Ellström M, Smits M, Rineau F, Canbäck B, Floudas D,
528 Carleer R, Lackner G, Braesel J, Hoffmeister D, Henrissat B, Ahrén D, Johansson T,
529 Hibbett DS, Martin F, Persson P, Tunlid A. 2016. Ectomycorrhizal fungi decompose soil
530 organic matter using oxidative mechanisms adapted from saprotrophic ancestors. New
531 Phytol **209**:1705-1719.
- 532 24. Fernandez-Fueyo E, Ruiz-Duenas FJ, Ferreira P, Floudas D, Hibbett DS, Canessa P,
533 Larrondo LF, James TY, Seelenfreund D, Lobos S, Polanco R, Tello M, Honda Y,
534 Watanabe T, Watanabe T, Ryu JS, Kubicek CP, Schmoll M, Gaskell J, Hammel KE, St
535 John FJ, Vanden Wymelenberg A, Sabat G, Splinter BonDurant S, Syed K, Yadav JS,
536 Doddapaneni H, Subramanian V, Lavin JL, Oguiza JA, Perez G, Pisabarro AG, Ramirez L,
537 Santoyo F, Master E, Coutinho PM, Henrissat B, Lombard V, Magnuson JK, Kues U, Hori
538 C, Igarashi K, Samejima M, Held BW, Barry KW, LaButti KM, Lapidus A, Lindquist EA,
539 Lucas SM, Riley R, Salamov AA, Hoffmeister D, Schwenk D, Hadar Y, Yarden O, de Vries
540 RP, Wiebenga A, Stenlid J, Eastwood D, Grigoriev IV, Berka RM, Blanchette RA, Kersten

- 541 **P, Martinez AT, Vicuna R, Cullen D.** 2012. Comparative genomics of *Ceriporiopsis*
542 *subvermispora* and *Phanerochaete chrysosporium* provide insight into selective
543 ligninolysis. *Proc Natl Acad Sci USA* **109**:5458-5463.
- 544 25. **Edgar RC.** 2004. MUSCLE: multiple sequence alignment with high accuracy and high
545 throughput. *Nucleic Acids Res* **32**:1792-1797.
- 546 26. **Oberegger H, Schoeser M, Zadra I, Abt B, Haas H.** 2001. SREA is involved in regulation of
547 siderophore biosynthesis, utilization and uptake in *Aspergillus nidulans*. *Mol Microbiol*
548 **41**:1077-1089.
- 549 27. **Schrettl M, Haas H.** 2011. Iron homeostasis--Achilles' heel of *Aspergillus fumigatus*? *Curr*
550 *Opin Microbiol* **14**:400-405.
- 551 28. **Schwecke T, Göttling K, Durek P, Duenas I, Kaufer NF, Zock-Emmenthal S, Staub E,**
552 **Neuhof T, Dieckmann R, von Döhren H.** 2006. Nonribosomal peptide synthesis in
553 *Schizosaccharomyces pombe* and the architectures of ferrichrome-type siderophore
554 synthetases in fungi. *ChemBioChem* **7**:612-622.
- 555 29. **Schrettl M, Bignell E, Kragl C, Sabiha Y, Loss O, Eisendle M, Wallner A, Arst HN, Jr.,**
556 **Haynes K, Haas H.** 2007. Distinct roles for intra- and extracellular siderophores during
557 *Aspergillus fumigatus* infection. *PLoS Pathog* **3**:1195-1207.
- 558 30. **Conti E, Stachelhaus T, Marahiel MA, Brick P.** 1997. Structural basis for the activation of
559 phenylalanine in the non-ribosomal biosynthesis of gramicidin S. *EMBO J* **16**:4174-4183.
- 560 31. **Stachelhaus T, Mootz HD, Marahiel MA.** 1999. The specificity conferring code of
561 adenylation domains in nonribosomal peptide synthetases. *Chem Biol* **6**:493-505.

- 562 32. **Lee TV, Johnson LJ, Johnson RD, Koulman A, Lane GA, Lott JS, Arcus VL.** 2010. Structure
563 of a eukaryotic nonribosomal peptide synthetase adenylation domain that activates a
564 large hydroxamate amino acid in siderophore biosynthesis. *J Biol Chem* **285**:2415-2427.
- 565 33. **Jalal MAF, Galles JL, Vanderhelm D.** 1985. Structure of Des(Diserylglycyl)Ferrirhodin,
566 Ddf, a Novel Siderophore from *Aspergillus ochraceous*. *J Org Chem* **50**:5642-5645.
- 567 34. **Diekmann H.** 1967. Stoffwechselprodukte von Mikroorganismen. 56. Mitteilung. Fusigen
568 – ein neues Sideramin aus Pilzen. *Arch Microbiol* **58**:1-5.
- 569 35. **Gao X, Haynes SW, Ames BD, Wang P, Vien LP, Walsh CT, Tang Y.** 2012. Cyclization of
570 fungal nonribosomal peptides by a terminal condensation-like domain. *Nat Chem Biol*
571 **8**:823-830.
- 572 36. **Krasnoff SB, Keresztes I, Donzelli BG, Gibson DM.** 2014. Metachelins, mannosylated
573 and *N*-oxidized coprogen-type siderophores from *Metarhizium robertsii*. *J Nat Prod* **77**:
574 1685-1692.
- 575 37. **Fischbach MA, Lin H, Liu DR, Walsh CT.** 2006. How pathogenic bacteria evade
576 mammalian sabotage in the battle for iron. *Nat Chem Biol* **2**:132-138.
- 577 38. **Blatzer M, Schrettl M, Sarg B, Lindner HH, Pfaller K, Haas H.** 2011. SidL, an *Aspergillus*
578 *fumigatus* transacetylase involved in biosynthesis of the siderophores ferricrocin and
579 hydroxyferricrocin. *Appl Environ Microbiol* **77**:4959-4966.
- 580 39. **Haselwandter K, Häninger G, Ganzera M.** 2011. Hydroxamate siderophores of the
581 ectomycorrhizal fungi *Suillus granulatus* and *S. luteus*. *Biometals* **24**:153-157.

- 582 40. **Keating TA, Suo Z, Ehmann DE, Walsh CT.** 2000. Selectivity of the yersiniabactin
583 synthetase adenylation domain in the two-step process of amino acid activation and
584 transfer to a holo-carrier protein domain. *Biochemistry* **39**:2297-2306.
- 585 41. **Sambrook J, Russell DW.** 2000. *Molecular Cloning: A Laboratory Manual*, 3rd ed., Cold
586 Spring Harbor Laboratory Press, Cold Spring Harbor.
- 587 42. **Gressler M, Hortschansky P, Geib E, Brock M.** 2015. A new high-performance
588 heterologous fungal expression system based on regulatory elements from the
589 *Aspergillus terreus* terrein gene cluster. *Front Microbiol* **6**:184.
- 590 43. **Shimizu K, Keller NP.** 2001. Genetic involvement of a cAMP-dependent protein kinase in
591 a G protein signaling pathway regulating morphological and chemical transitions in
592 *Aspergillus nidulans*. *Genetics* **157**:591-600.
- 593 44. **Sanchez C, Du L, Edwards DJ, Toney MD, Shen B.** 2001. Cloning and characterization of
594 a phosphopantetheinyl transferase from *Streptomyces verticillus* ATCC15003, the
595 producer of the hybrid peptide-polyketide antitumor drug bleomycin. *Chem Biol* **8**:725-
596 738.
- 597 45. **Bradford MM.** 1976. A rapid and sensitive method for the quantitation of microgram
598 quantities of protein utilizing the principle of protein-dye binding. *Anal Biochem* **72**:248-
599 254.
- 600 46. **Schwyn B, Neilands JB.** 1987. Universal CAS assay for the detection and determination
601 of siderophores. *Anal Biochem* **160**:47-60.

- 602 47. **Shin SH, Lim Y, Lee SE, Yang NW, Rhee JH.** 2001. CAS agar diffusion assay for the
603 measurement of siderophores in biological fluids. *J Microbiol Methods* **44**:89-95.
- 604 48. **Milagres AM, Machuca A, Napoleao D.** 1999. Detection of siderophore production from
605 several fungi and bacteria by a modification of chrome azurol S (CAS) agar plate assay. *J*
606 *Microbiol Methods* **37**:1-6.
- 607 49. **Schneider P, Weber M, Rosenberger K, Hoffmeister D.** 2007. A one-pot
608 chemoenzymatic synthesis for the universal precursor of antidiabetes and antiviral bis-
609 indolylquinones. *Chem Biol* **14**:635-644.
- 610 50. **Tamura K, Peterson P, Peterson N, Stecher G, Nei M, Kumar S.** 2011. MEGA5: molecular
611 evolutionary genetics analysis using maximum likelihood, evolutionary distance, and
612 maximum parsimony methods. *Mol Biol Evol* **28**:2731-2739.
- 613 51. **Lin YM, Miller MJ.** 1999. Practical synthesis of hydroxamate-derived siderophore
614 components by an indirect oxidation method and syntheses of a DIG-siderophore
615 conjugate and a biotin-siderophore conjugate. *J Org Chem* **64**:7451-7458.
- 616 52. **Lee BN, Kroken S, Chou DY, Robbertse B, Yoder OC, Turgeon BG.** 2005. Functional
617 analysis of all nonribosomal peptide synthetases in *Cochliobolus heterostrophus* reveals
618 a factor, NPS6, involved in virulence and resistance to oxidative stress. *Eukaryot Cell*
619 **4**:545-555.
- 620 53. **Kohler A, Kuo A, Nagy LG, Morin E, Barry KW, Buscot F, Canbäck B, Choi C, Cichocki N,**
621 **Clum A, Colpaert J, Copeland A, Costa MD, Doré J, Floudas D, Gay G, Girlanda M,**
622 **Henrissat B, Herrmann S, Hess J, Högberg N, Johansson T, Khouja HR, LaButti K,**

623 **Lahrmann U, Levasseur A, Lindquist EA, Lipzen A, Marmeisse R, Martino E, Murat C,**
624 **Ngan CY, Nehls U, Plett JM, Pringle A, Ohm RA, Perotto S, Peter M, Riley R, Rineau F,**
625 **Ruytinx J, Salamov A, Shah F, Sun H, Tarkka M, Tritt A, Veneault-Fourrey C, Zuccaro A;**
626 **Mycorrhizal Genomics Initiative Consortium., Tunlid A, Grigoriev IV, Hibbett DS,**
627 **Martin F.** 2015. Convergent losses of decay mechanisms and rapid turnover of symbiosis
628 genes in mycorrhizal mutualists. *Nat Genet* **47**:410-415.

629

630 **FIGURE LEGENDS**

631 **Fig. 1.** Chemical structures of fungal siderophores. Abbreviations: DDF:
632 des(diserylglycl)ferrirhodin; TAFC: triacetylfulvarinine C.

633

634 **Fig. 2.** Physical map of basidioferrin biosynthetic genes in *Ceriporiopsis subvermispora*. The
635 black arrows represent the transcriptional direction of the *CsNPS2* and *SMO1* genes. Intron
636 positions within the genes are indicated by spaces between arrow segments. Below: domain
637 setup of *CsNPS2*. Domain abbreviations are: A, adenylation; C, condensation; T, thiolation.

638

639 **Fig. 3.** Neighbor-joining tree of adenylation domains of selected fungal siderophore
640 synthetases. Organism and enzyme names, accession numbers, as well as the number of the A
641 domain (i.e. A1-A3 in case of multiple A domains per enzyme) are indicated on leaves. *CsNPS2*
642 belongs to the monophyletic type VI clade, a subclade of *N*⁵-acyl-*N*⁵-hydroxy-L-ornithine (Acyl-
643 HO) activating A domains and exclusively consists of basidiomycete sequences. Bootstrap
644 values above 50% are shown above branches. The scale bar represents the number of amino
645 acid substitutions per site. The branch to *Omphalotus olearius* Fso1 A3 is not drawn to scale.
646 Accession numbers refer to entries in the NCBI, PDB, or the JGI database (protein IDs) of the
647 Joint Genome Institute.

648

649 **Fig. 4.** Adenylation domain substrate specificity of *Ceriporiopsis subvermispora* *CsNPS2*
650 siderophore synthetase, determined by the ATP-[³²P]pyrophosphate radioisotope exchange

651 assay. Abbreviations: cpm: counts per minute; L-AHO, N^5 -acetyl- N^5 -hydroxy-L-ornithine; L-
652 AMHO, N^5 -*cis*-anhydromevalonyl- N^5 -hydroxy-L-ornithine; Error bars indicate the standard
653 deviation of three independent experiments.

654

655 **Fig. 5.** HPLC analysis ($\lambda = 210$ nm) of CsNPS2-dependent basidioferrin production *in vitro*.
656 Negative control: ATP-omitted reaction. The high-resolution mass spectrum (positive mode)
657 refers to the signal at $t_R = 8.3$ min, which corresponds to basidioferrin (chemical structure top
658 left).

659

660

661

662

663

664 **Table 1:** Comparison of fungal siderophore synthetases mentioned in this study with CsNPS2 and like enzymes. For synthetases
665 featuring more than one A domain, it is indicated in brackets to which A domain the NRPS code and substrate specificity refer.
666 Abbreviations: L-AHO, *N*⁵-acetyl-*N*⁵-hydroxy-L-ornithine; L-AMHO, *N*⁵-*cis*-anhydromevalonyl-*N*⁵-hydroxy-L-ornithine; L-MGHO,
667 *N*⁵-*trans*-(α -methyl)-glutaconyl-*N*⁵-hydroxy-L-ornithine. Domain abbreviations: A, adenylation; dA, degenerate adenylation; C,
668 condensation; T, thiolation. The siderophore synthetase categories described by Turgeon and co-workers [3] are given in the
669 column "synthetase type".

670

671

672

673

674

675

676

677

678

Synthetase type	Organism	NRPS (A domain)	Synthetase domain structure	NRPS code	Substrate	Ref.
I	<i>Ustilago maydis</i>	Sid2 (A2)	A-T-C-A-T-C-A-T-C-T-C	DVLSIGAIGK	L-AHO	[16]
I	<i>Ustilago maydis</i>	Sid2 (A3)	A-T-C-A-T-C-A-T-C-T-C	DVIDMGAIGK	L-AHO	[16]
II	<i>Neotyphodium lolii</i>	SidN (A3)	A-T-C-A-T-C-A-T-C-T-C-T-C	DVGGGGVIGK	L-AMHO	[32]
II	<i>Aspergillus fumigatus</i>	SidC (A3)	A-T-C-A-T-C-A-T-C-T-C-T-C	DVLSSGAIGK	L-AHO	[8]
II	<i>Omphalotus olearius</i>	Fso1 (A3)	A-T-C-A-T-C-A-T-C-T-C-T-C	DIITITATLR	L-MGHO	[18]
II	<i>Ustilago maydis</i>	Fer3 (A3)	A-T-C-A-T-C-A-T-C-T-C-T-C	DVSSGGAIMK	L-MGHO	[17]
III	<i>Schizosaccharomyces pombe</i>	Sib1 (A3)	A-T-C-T-C-dA-T-C-A-T-C-T-C-T-C	DVLDIGFIGK	L-AHO	[28]
V	<i>Cochliobolus heterostrophus</i>	NPS2 (A4)	A-T-C-A-T-C-A-T-C-A-T-C-T-C-T-C	DVLDIGGIGK	L-AHO	[3,52]
VI	<i>Coniophora puteana</i>	NPS1	A-T-C-T-C-T-C	DVSGAGFIGK	?	[20]
VI	<i>Serpula lacrymans</i>	NPS4	A-T-C-T-C-T-C	DVCGGGFIGK	?	[21]
VI	<i>Coprinopsis cinerea</i>	EAU88504.2	A-T-C-T-C-T-C	DVCGGGFIGK	?	[22]
VI	<i>Suillus luteus</i>	Sid1	A-T-C-T-C-T-C	DVAGAGFIGK	?	[53]
VI	<i>Stereum hirsutum</i>	EIM88654.1	A-T-C-T-C-T-C	DVSGVGFVGK	?	[20]
VI	<i>Fomitiporia mediterranea</i>	EJD05778.1	A-T-C-T-C-T-C	DVAGAGFIGK	?	[20]
VI	<i>Ceriporiopsis subvermispora</i>	CsNPS2	A-T-C-T-C-T-C	DVAGAGFIGK	L-AHO	[24, this work]

679

680

681

682

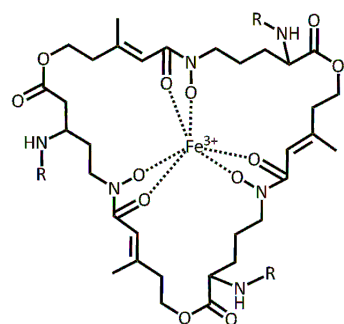
683

684

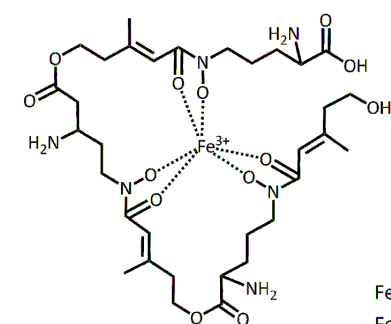
685 **Table 2.** Sequences (5' to 3') of oligonucleotide primers.

Primer	Sequence
NPS2-1	CGGAGCCAGCTCTAAGAGAAC
NPS2fw	TTATGGCGGATCCAATGAGCGCACAC
NPS2rev	GTGTCTGAATTCACGGAGCGTTATAGGATTCC
oRL1	CTAGAAGTGATTGGCCGTATCG
oRL2	CTAACCCGCGACTCAATTGATTCTG
oEB28	CATCACAGCACCATGCGGGTTCTCATCATCATCATC
oEB30	ATCACTGCTGCCATGGCTAAGCAAGGCACTCCTTGAC
oRL3	CATACCGAACTGGCGATCTC
oRL4	CGGAGCCAGCTCTAAGAGAAC
oEB46	TCAAGTACGACTCCGTCCAC
oEB47	GTACCACGAGATGAGCTTG
oEB48	GTGTGAAGAAGGTCGAGG
oEB49	GTCTGCGTAGACGAGAAG
oEB54	GGAAGCACAAGATCCTCTG
oEB55	GTTGCGGAGTCTGTTTCG
oRL5	CATACCGAACTGGCGATCTC
oRL6	CGGAGCCAGCTCTAAGAGAAC
2641	GACGGCCAGTGAATTCGATCCTCTCTGATATTGTCG
2644	TACCGAGCTCGAATTCGAGTGAGGGTTGAGTACGAG

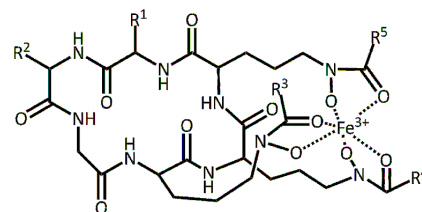
686



TAFC: R = COCH₃
Fusigen: R = H



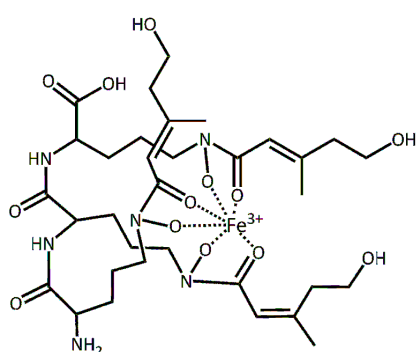
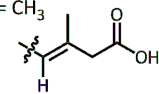
Fusarinine B



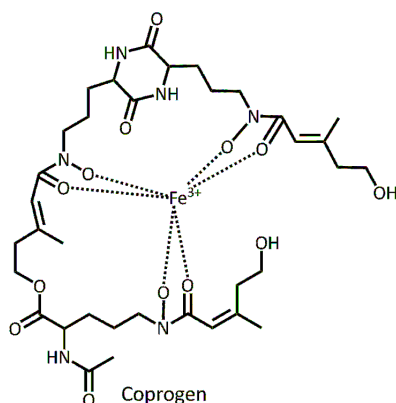
Ferrichrome: R¹ = R² = H, R³ = R⁴ = R⁵ = CH₃

Ferricrocin: R¹ = H, R² = CH₂OH, R³ = R⁴ = R⁵ = CH₃

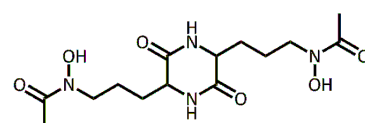
Ferrichrome A: R¹ = R² = CH₂OH, R³ = R⁴ = R⁵ =



DDF



Coprogen



Rhodotorulic Acid

